GEOLOGY | THE GEOLOGICAL SOCIETY OF AMERICA®

https://doi.org/10.1130/G48647.1

Manuscript received 19 November 2020
Revised manuscript received 27 February 2021
Manuscript accepted 4 March 2021

Diapiric relamination of the Orocopia Schist (southwestern U.S.) during low-angle subduction

James B. Chapman
Department of Geology and Geophysics, University of Wyoming, Laramie, Wyoming 82701, USA

ABSTRACT

The Orocopia Schist and related schists are sediments subducted during the Laramide orogeny and are thought to have been underplated as a laterally extensive layer at the base of the crust in the southwestern United States Cordillera. This concept is hard to reconcile with the existence of continental mantle lithosphere in southeastern California and western Arizona. Analytical solutions and numerical modeling suggest that the Orocopia Schist may have ascended through the mantle lithosphere as sediment diapirs or subsolidus crustal plumes to become emplaced in the middle to lower crust. Modeled time-temperature cooling paths are consistent with the exhumation history of the Orocopia Schist and explain an initial period of rapid cooling shortly after peak metamorphism. The Orocopia Schist represents a potential example of relaminated sediment observable at the surface.

INTRODUCTION

Shallow to flat-slab subduction is one of the primary causes of large-scale sediment subduction, during which trench, accretionary complex, and forearc basin material is tectonically eroded and transported beneath the upper plate (Ducea and Chapman, 2018). The fate of this subducted crustal material has global implications for the composition and evolution of the lithosphere, and such material may be recycled into the mantle, underplated, or relaminated (Clift and Vannucchi, 2004; Behn et al., 2011; Hacker et al., 2011; Kelemen and Behn, 2016). In the southern United States Cordillera, shallow subduction during the Laramide orogeny resulted in the sublithospheric emplacement of the Pelona, Rand, Orocopia, San Emigdio, and Sierra de Salinas schists, which were subsequently exhumed to the surface during the late Cenozoic (Chapman, 2017). Current models propose that these schists were emplaced as a laterally extensive sheet beneath the crust (e.g., Jacobson et al., 2007). These models are supported by outcrops near the paleo–plate margin where the schists are demonstrably underplated directly to the base of the crust and contributed to extinguishing the Late Cretaceous Sierra Nevada continental arc (Kidder and Ducea, 2006). Farther inland, however, the emplacement mechanism of these schists is less certain. Recent discoveries of Orocopia Schist in western Arizona (Haxel et al., 2015; Jacobson et al., 2017; Strickland et al., 2018) expanded the landward limit for known schist emplacement (Fig. 1). Models suggesting that a sheet of Orocopia Schist was underplated to the crust imply that mantle lithosphere was removed during low-angle subduction. However, mantle xenolith, isotopic, and geophysical studies indicate the mantle lithosphere was not fully removed during the Laramide orogeny in the southwestern United States (Livaccari and Perry, 1993; DePaolo and Daley, 2000; Allison et al., 2013), and structural restorations and thermochronologic data indicate that the Orocopia Schist was emplaced in the lower to middle crust shortly after peak metamorphism but prior to late Cenozoic exhumation (Jacobson et al., 2007; Spencer et al., 2018; Strickland et al., 2018). These observations beg the question: after the Orocopia Schist was subducted, how did it come to reside in the crust if the mantle lithosphere and possibly lower crust were in its way?

EMPLACEMENT CONDITIONS OF THE OROCOPIA SCHIST

The events associated with the emplacement of the Orocopia and related schists resulted in the dismemberment and destruction of the plate margin, including nearly complete removal of a massive accretionary complex and forearc basin (Jacobson et al., 2011). These schists are estimated to have subducted as a 10 ± 5-km-thick layer based on outcrop exposures, structural reconstructions, and low-velocity anomalies in the middle to lower crust (Porter et al., 2011; Xia and Platt, 2017; Spencer et al., 2018). This detail alone distinguishes the Orocopia Schist from most other documented instances of sediment subduction that have subducted layer thicknesses of $\leq$1 km (Clift and Vannucchi, 2004). Layer thickness is a critical length scale that determines how rapidly and at what rheological conditions sediment detaches from the downgoing slab. Sediment diapirs are proposed to form for any sediment layer thicker than ~300 m at temperatures as low as 500 °C (Currie et al., 2007; Behn et al., 2011; Miller and Behn, 2012).

Peak metamorphic conditions recorded by the Orocopia Schist are 0.8–1.4 GPa and 550–650 °C (Chapman, 2017). New maximum temperature estimates using Raman spectroscopy of carbonaceous material in the Orocopia Schist from recently discovered locations in western Arizona are 599–649 °C at Cemetery Ridge and 546–583 °C at the Plomosa Mountains (Table S1 in the Supplemental Material[1]). Phase modeling of subducted metasedimentary rocks at these pressure-temperature conditions (Behn et al., 2011) indicates a density contrast of ~550 kg/m^3 between the Orocopia Schist and the continental mantle lithosphere and a density contrast of up to 200 kg/m^3 with the lower crust. Density contrasts as low as 100 kg/m^3 have been linked to instability growth (Currie et al., 2007; Behn et al., 2011).

Viscosity also influences the formation of density instabilities and is largely dependent on temperature and strain rate. Strain rates as

[1]Supplemental Material. Raman spectroscopy of carbonaceous material (RSCM) results and details of numerical models. Please visit https://doi.org/10.1130/GEOL.S.14390711 to access the supplemental material, and contact editing@geosociety.org with any questions.

CITATION: Chapman, J.B., 2021, Diapiric relamination of the Orocopia Schist (southwestern U.S.) during low-angle subduction: Geology, v. 49, p. , https://doi.org/10.1130/G48647.1

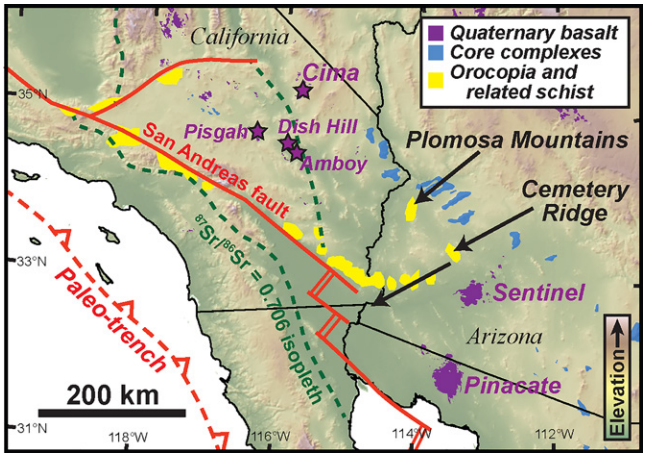

Figure 1. Regional map of the southwest United States Cordillera showing outcrops of Orocopia and related schists. Geophysical studies suggest that mantle lithosphere is present east of the Pisgah and Cima volcanic fields in California (Allison et al., 2013), and isotopic studies suggest mantle lithosphere is present east of 116°–115°W longitude (Miller et al., 2000; Chapman et al., 2018). Base map is a 1-arc-second digital elevation model from the U.S. Geological Survey.

high 10^{-13} s^{-1} have been reported from the Pelona Schist based on deformed quartz fabrics (Xia and Platt, 2017). Strain rate in the continental mantle lithosphere near the slab interface in the region of flat-slab subduction has been estimated at 10^{-15} to 10^{-16} s^{-1} based on the results of numerical modeling (Liu and Currie, 2019). At these strain rates and temperatures (550–650°C), the wet quartzite flow law of Hirth et al. (2001) suggests that the Orocopia Schist had an effective viscosity of 10^{19} to 10^{21} Pa·s. The lower end of this range is comparable to values modeled for lower crustal flow (e.g., Beaumont et al., 2001). Post-seismic relaxation and xenolith studies from the area underlain by the Orocopia Schist indicate that modern mantle lithosphere has an effective viscosity of 10^{19} to 10^{20} Pa·s (Behr and Hirth, 2014). Laramide-age upper mantle xenoliths from the stable Colorado Plateau indicate effective viscosities of 10^{19} to 10^{23} Pa·s at 550–750 °C and an assumed pressure of 2 GPa (Behr and Smith, 2016). Analytical solutions for Rayleigh-Taylor instabilities in two-layer systems (Hess and Parmentier, 1995) applied to the Orocopia Schist and the mantle lithosphere at the conditions described produce characteristic instability growth times of 0.5–5 m.y., diapir diameters of 30–80 km, and maximum ascent velocities of 0.1–2 km/m.y., assuming a 10-km-thick layer of schist (Fig. 2).

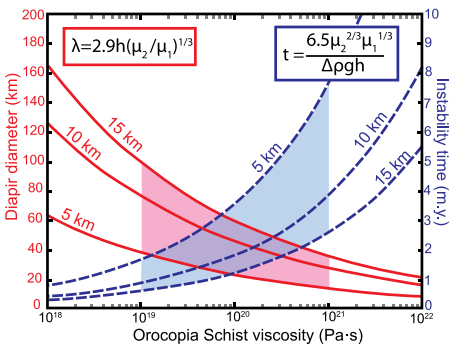

Figure 2. Analytical solutions for characteristic wavelength, λ, and instability time, *t*, for diapir formation in a two-layer system with variable lower-layer (Orocopia Schist) thickness, *h*, and viscosity, μ_1. The viscosity of the upper layer, μ_2 (mantle lithosphere), is 10^{21} Pa·s, and the density difference, Δρ, of the two layers is 550 kg/m³.

Reconstructed time-temperature histories for the Orocopia Schist indicate that subduction, prograde to peak metamorphism, and initial cooling all occurred in <15 m.y. (Grove et al., 2003; Jacobson et al., 2007, 2011) (Fig. 3). The period of initial cooling (Fig. 3) is enigmatic and has been variably attributed to erosional exhumation, thrust faulting, extensional faulting, isostacy, and subduction channel return flow (Chapman, 2017). Rapid initial cooling to 300–400 °C supports emplacement of the Orocopia Schist in the lower to middle crust, where it resided for 20–50 m.y. before being exhumed to the surface during the Miocene (Fig. 3). The most extreme example of crustal emplacement comes from the Plomosa Mountains, where the Orocopia Schist may have been located as shallow as 5 km prior to exhumation (Spencer et al., 2018; Strickland et al., 2018). I propose that the period of rapid initial cooling can be explained by diapiric ascent of the Orocopia Schist from the Farallon slab to the middle crust.

NUMERICAL EXPERIMENTS AND MODEL SETUP

To explore the possibility of relamination, I consider two end-member numerical models involving density instabilities that can place the Orocopia Schist above the mantle lithosphere (Fig. 4). Model 1 is inspired by studies that suggest isotherms are nearly parallel to the plate interface in flat-slab segments (e.g., Liu and Currie, 2019) and supposes that several discrete instabilities formed nearly simultaneously (Chapman, 2017). Model 2 supposes that instability growth is a direct function of temperature and depth and that the Orocopia Schist detached from the Farallon slab at a point-like source in a fixed upper plate reference frame. This model is broadly analogous to the "extrusion" model that Strickland et al. (2018) proposed for the Plomosa Mountains or the more general "crustal plume" model of Currie et al. (2007). Model 2 introduces Orocopia Schist–like material into the bottom left of the model at a rate of 10 cm/yr, consistent with conservative estimates of the North America–Farallon plate convergence rate during the Laramide orogeny (Torsvik et al., 2008).

The numerical experiments were conducted using the finite-element software COMSOL Multiphysics (https://www.comsol.com/comsol-multiphysics). Figure 4B describes the geometry and initial conditions for a reference model based on the thickness, density, viscosity, temperature, and pressure constraints outlined above. The thickness of the mantle lithosphere is constrained by maximum pressure estimates from metamorphic studies (Chapman, 2017, and references therein). The initial geotherm was scaled to match the thermal structure of numerical models of flat-slab subduction at 50–110 km depth that suggest a slab-mantle interface of ~600 °C (Liu and Currie, 2019), consistent with peak metamorphic temperatures. Internal heat generation, strain heating, and adiabatic heating were neglected. The density and viscosity of layers representing the crust and Orocopia Schist were coupled to the thermal model and varied as a function of temperature using the wet quartz flow law of Hirth et al. (2001). Model details are presented in the Supplemental Material.

GENERATION AND CHARACTERISTICS OF SEDIMENT DIAPIRS

The numerical modeling results predict diapiric rise of the Orocopia Schist at the conditions considered. Figures 4C and 4D show model results at intermediate time steps using

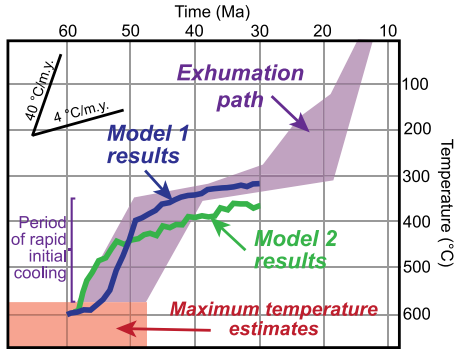

Figure 3. Comparison of observed cooling history of the Orocopia Schist (Grove et al., 2003; Jacobson et al., 2007, 2011) with time-temperature paths generated by numerical modeling of sediment diapirism. Models are consistent with a period of rapid initial cooling from peak metamorphic conditions (~600 °C) to 300–400 °C, which is interpreted to represent lower to middle crustal depths.

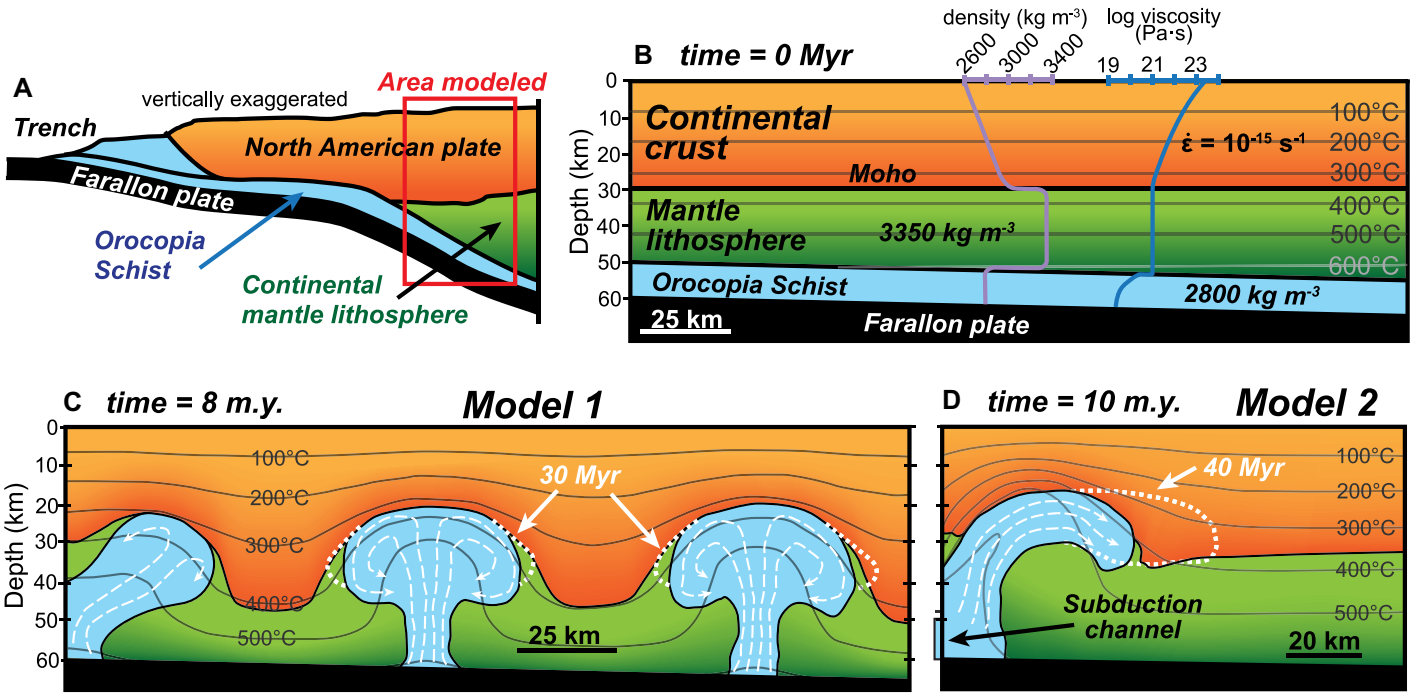

Figure 4. (A) Schematic cross section showing subduction of Orocopia Schist beneath mantle lithosphere. (B) Reference model geometry showing temperature, density, and viscosity variations with depth. $\dot{\varepsilon}$ strainis strain rate. (C) Results of model 1 at time *t* = 8 m.y. showing diapir formation. (D) Results of model 2 at *t* = 10 m.y. showing "crustal plume." Heavy dashed white lines show the position of "Orocopia Schist" at subsequent time steps. Thinner, dashed white lines are schematic flow lines.

the starting conditions described in the reference model. Both model 1 and model 2 produce large-scale diapir-like features that become emplaced in the lower to middle crust (as shallow as 20 km depth) in <10 m.y. Model 1 generates classic Rayleigh-Taylor instabilities that reach a maximum diameter of ~65 km after emplacement (Fig. 4C). The lower crust is thickened between the instabilities. Model 2 produces a plume-like structure that rises rapidly into the middle crust and then starts to grow horizontally for as long as Orocopia Schist is input into the model. The position of the plume at the end of the model run is shown in Figure 4D. The "crustal plume" exhibits only minor vertical thickening during its lateral growth. The lower crust is thickened in front of the growing plume.

Tens of model trials were run for model 1, deviating from the reference model to explore variations in subducted sediment thickness and viscosity, which is affected primarily by temperature and strain rate. Sedimentary diapirs continued to be produced with a layer thickness of 1 km, the smallest thickness considered. Increasing the maximum mantle lithosphere viscosity to 10^{22} Pa·s delayed instability development (~40 m.y. after the start of a model run), and increasing the mantle lithosphere viscosity to 10^{23} Pa·s failed to produce instabilities in a 100-m.y.-long model run. Increasing the maximum viscosity of the Orocopia Schist layer to 10^{21} Pa·s delayed instability formation by 2–3 m.y. but otherwise had little effect on diapir generation. This analysis suggests that mantle lithosphere viscosity has the largest effect on the development of sediment diapirs and represents the greatest uncertainty within the model parameters considered.

Thermal models for subduction zones suggest that mantle temperatures initially increase upward from the slab, reaching a peak in the core of the mantle wedge, which may facilitate the formation of diapirs (e.g., Jull and Kelemen, 2001; Miller and Behn, 2012). During flat-slab subduction, where no asthenospheric mantle is present between the slab and the lithosphere, temperature inversions within the lithospheric mantle are predicted to be subdued (e.g., Liu and Currie, 2019) but may still enhance diapirism. The addition of a "hot core" to the mantle lithosphere in model 1 (~150 °C above the ambient geotherm) was investigated using a wet olivine flow law for viscosity (Hirth and Kohlstedf, 2003) but did not produce significantly different results compared to model runs without the "hot core." The relatively thin mantle lithosphere in model 1 (20–30 km) limited viscous decay caused by temperature gradients.

The temperature of the sediment diapirs was tracked to compare the model results with observed time-temperature histories of Orocopia Schist (Fig. 3). Model 1 indicates rapid cooling (~40 °C/m.y.) during initial ascent of the instability and then a step-like shift to slow cooling (3–5 °C/m.y.) for the remainder of the model run as the diapir slowly equilibrates to the ambient geotherm. The shape of the cooling path and the final temperature of the modeled sediment diapir in model 1 are consistent with the observed time-temperature paths (Fig. 3). Model 2 also indicates initial rapid cooling (~35 °C/m.y.) during diapir ascent, but the cooling rate gradually slows through time until it reaches a cooling rate similar to that of model 1 (3–5 °C/m.y.).

DISCUSSION AND CONCLUSIONS

The Orocopia Schist, cropping out at the surface of Earth and located as much as 450 km from the paleo-trench (present-day coordinates), is one of the most unambiguous examples of subducted sediment being reincorporated into the crust. The thickness, density, and rheology of the Orocopia Schist suggest that it was susceptible to the formation of sediment diapirs if subducted beneath the lithospheric mantle.

However, the possibility of relatively high viscosities ($\geq 10^{23}$ Pa·s) in the upper mantle may limit the applicability of diapir models. The wet olivine flow law of Hirth and Kohlstedf (2003) predicts upper mantle viscosities of 10^{23} to 10^{25} Pa·s at the strain rate and temperatures considered—higher than required by the modeling results ($<10^{22}$ Pa·s). The modeled values overlap with viscosity estimates determined from Laramide-age mantle xenoliths (10^{19} to 10^{23} Pa·s), but these xenoliths came from the deepest, most viscous parts of the lithosphere (Behr and Smith, 2016). Lithospheric mantle xenoliths from southern California have diverse mineralogy and exhibit evidence for metasomatic alteration (Luffi et al., 2009; Chin et al., 2014), which suggests that viscosities calculated assuming a

homogenous olivine composition are maximum estimates. Another possibility is that preexisting structural heterogeneities may have focused buoyant ascent of the Orocopia Schist.

Analytical solutions for Rayleigh-Taylor instabilities in two-layer systems (Fig. 2) and numerical models (Fig. 4) suggest that Orocopia Schist would have detached from the Farallon slab as diapirs or subsolidus crustal plumes and ascended through the mantle lithosphere and into the lower crust—a form of relamination. Time-temperature cooling paths produced from the numerical models are consistent with the observed exhumation history of the Orocopia Schist and may explain a period of rapid initial cooling (Fig. 3). Diapirism is consistent with mechanical mixing of mantle rocks (peridotite, actinolite and/or tremolite pods) and schist observed at Cemetery Ridge and the Plomosa Mountains (Haxel et al., 2015; Strickland et al., 2018).

The results suggest that conceptual models for a laterally extensive sheet of Orocopia Schist lying below the base of the crust throughout the southwestern United States may be unrealistic, particularly where mantle lithosphere is still present (e.g., Allison et al., 2013). The emplacement mechanisms proposed here predict that Orocopia Schist should be nonuniform and localized in the subsurface. The counterpart to rising diapirs of Orocopia Schist are descending "drips" of mantle lithosphere that may have been prone to delamination after the removal of the Farallon plate. This could help to explain a long-standing issue related to the discontinuous and patchwork-like preservation of mantle lithosphere in the southwestern U.S. Cordillera (e.g., Livacarri and Perry, 1993). Finally, the modeling predicts crustal thickening roughly equivalent to the thickness of the subducted sediment layer. The emplacement of the Orocopia Schist may help explain significant crustal thickening during the Laramide orogeny in southern Arizona, which cannot be explained by horizontal shortening alone (Chapman et al., 2020).

ACKNOWLEDGMENTS

This work was supported by U.S. National Science Foundation grant EAR-1928312. Constructive reviews by Claire Currie, Carl Jacobson, and Greg Hirth improved the manuscript.

REFERENCES CITED

Allison, C.M., Porter, R.C., Fouch, M.J., and Semken, S., 2013, Seismic evidence for lithospheric modification beneath the Mojave Neovolcanic Province, Southern California: Geophysical Research Letters, v. 40, p. 5119–5124, https://doi.org/10.1002/grl.50993.

Beaumont, C., Jamieson, R.A., Nguyen, M.H., and Lee, B., 2001, Himalayan tectonics explained by extrusion of a low-viscosity crustal channel coupled to focused surface denudation: Nature, v. 414, p. 738–742, https://doi.org/10.1038/414738a.

Behr, W.M., and Hirth, G., 2014, Rheological properties of the mantle lid beneath the Mojave region in southern California: Earth and Planetary Science Letters, v. 393, p. 60–72, https://doi.org/10.1016/j.epsl.2014.02.039.

Behr, W.M., and Smith, D., 2016, Deformation in the mantle wedge associated with Laramide flat-slab subduction: Geochemistry Geophysics Geosystems, v. 17, p. 2643–2660, https://doi.org/10.1002/2016GC006361.

Behn, M.D., Kelemen, P.B., Hirth, G., Hacker, B.R., and Massonne, H.-J., 2011, Diapirs as the source of the sediment signature in arc lavas: Nature Geoscience, v. 4, p. 641–646, https://doi.org/10.1038/ngeo1214.

Chapman, A.D., 2017, The Pelona–Orocopia–Rand and related schists of southern California: A review of the best-known archive of shallow subduction on the planet: International Geology Review, v. 59, p. 664–701, https://doi.org/10.1080/00206814.2016.1230836.

Chapman, J.B., Dafov, M.N., Gehrels, G., Ducea, M.N., Valley, J.W., and Ishida, A., 2018, Lithospheric architecture and tectonic evolution of the southwestern U.S. Cordillera: Constraints from zircon Hf and O isotopic data: Geological Society of America Bulletin, v. 130, p. 2031–2046, https://doi.org/10.1130/B31937.1.

Chapman, J.B., Greig, R., and Haxel, G.B., 2020, Geochemical evidence for an orogenic plateau in the southern U.S. and northern Mexican Cordillera during the Laramide orogeny: Geology, v. 48, p. 164–168, https://doi.org/10.1130/G47117.1.

Chin, E.J., Lee, C.-T.A., and Barnes, J.D., 2014, Thickening, refertilization, and the deep lithosphere filter in continental arcs: Constraints from major and trace elements and oxygen isotopes: Earth and Planetary Science Letters, v. 397, p. 184–200, https://doi.org/10.1016/j.epsl.2014.04.022.

Clift, P., and Vannucchi, P., 2004, Controls on tectonic accretion versus erosion in subduction zones: Implications for the origin and recycling of the continental crust: Reviews of Geophysics, v. 42, RG2001, https://doi.org/10.1029/2003RG000127.

Currie, C.A., Beaumont, C., and Huismans, R.S., 2007, The fate of subducted sediments: A case for backarc intrusion and underplating: Geology, v. 35, p. 1111–1114, https://doi.org/10.1130/G24098A.1.

DePaolo, D.J., and Daley, E.E., 2000, Neodymium isotopes in basalts of the southwest basin and range and lithospheric thinning during continental extension: Chemical Geology, v. 169, p. 157–185, https://doi.org/10.1016/S0009-2541(00)00261-8.

Ducea, M.N., and Chapman, A.D., 2018, Sub-magmatic arc underplating by trench and forearc materials in shallow subduction systems; A geologic perspective and implications: Earth-Science Reviews, v. 185, p. 763–779, https://doi.org/10.1016/j.earscirev.2018.08.001.

Grove, M., Jacobson, C.E., Barth, A.P., and Vucic, A., 2003, Temporal and spatial trends of Late Cretaceous–early Tertiary underplating of Pelona and related schist beneath southern California and southwestern Arizona, *in*, Johnson, S.E., et al., eds., Tectonic Evolution of Northwestern Mexico and the Southwestern USA: Geological Society of America Special Paper 374, 26 p. 381–406, https://doi.org/10.1130/0-8137-2374-4.381.

Hacker, B.R., Kelemen, P.B., and Behn, M.D., 2011, Differentiation of the continental crust by relamination: Earth and Planetary Science Letters, v. 307, p. 501–516, https://doi.org/10.1016/j.epsl.2011.05.024.

Haxel, G.B., Jacobson, C.E., and Wittke, J.H., 2015, Mantle peridotite in newly discovered far-inland subduction complex, southwest Arizona: Initial report: International Geology Review, v. 57, p. 871–892, https://doi.org/10.1080/00206814.2014.928916.

Hess, P.C., and Parmentier, E.M., 1995, A model for the thermal and chemical evolution of the Moon's interior: Implications for the onset of mare volcanism: Earth and Planetary Science Letters, v. 134, p. 501–514, https://doi.org/10.1016/0012-821X(95)00138-3.

Hirth, G., and Kohlstedf, D., 2003, Rheology of the upper mantle and the mantle wedge: A view from the experimentalists, *in* Eiler, J., ed., Inside the Subduction Factory: American Geophysical Union Geophysical Monograph 138, p. 83–106, https://doi.org/10.1029/138GM06.

Hirth, G., Teyssier, C., and Dunlap, W.J., 2001, An evaluation of quartzite flow laws based on comparisons between experimentally and naturally deformed rocks: International Journal of Earth Sciences, v. 90, p. 77–87, https://doi.org/10.1007/s005310000152.

Jacobson, C.E., Grove, M., Vućić, A., Pedrick, J.N., and Ebert, K.A., 2007, Exhumation of the Orocopia Schist and associated rocks of southeastern California: Relative roles of erosion, syn-subduction tectonic denudation, and middle Cenozoic extension, *in* Cloos, M., et al., eds., Convergent Margin Terranes and Associated Regions: A Tribute to W.G. Ernst: Geological Society of America Special Paper 419, p. 1–37, https://doi.org/10.1130/2007.2419(01).

Jacobson, C.E., Grove, M., Pedrick, J.N., Barth, A.P., Marsaglia, K.M., Gehrels, G.E., and Nourse, J.A., 2011, Late Cretaceous–early Cenozoic tectonic evolution of the southern California margin inferred from provenance of trench and forearc sediments: Geological Society of America Bulletin, v. 123, p. 485–506, https://doi.org/10.1130/B30238.1.

Jacobson, C.E., Hourigan, J.K., Haxel, G.B., and Grove, M., 2017, Extreme latest Cretaceous–Paleogene low-angle subduction: Zircon ages from Orocopia Schist at Cemetery Ridge, southwestern Arizona, USA: Geology, v. 45, p. 951–954, https://doi.org/10.1130/G39278.1.

Jull, M., and Kelemen, P.A., 2001, On the conditions for lower crustal convective instability: Journal of Geophysical Research, v. 106, p. 6423–6446, https://doi.org/10.1029/2000JB900357.

Kelemen, P.B., and Behn, M.D., 2016, Formation of lower continental crust by relamination of buoyant arc lavas and plutons: Nature Geoscience, v. 9, p. 197–205, https://doi.org/10.1038/ngeo2662.

Kidder, S., and Ducea, M.N., 2006, High temperatures and inverted metamorphism in the schist of Sierra de Salinas, California: Earth and Planetary Science Letters, v. 241, p. 422–437, https://doi.org/10.1016/j.epsl.2005.11.037.

Liu, X., and Currie, C.A., 2019, Influence of upper plate structure on flat-slab depth: Numerical modeling of subduction dynamics: Journal of Geophysical Research: Solid Earth, v. 124, p. 13,150–13,167, https://doi.org/10.1029/2019JB018653.

Livaccari, R.F., and Perry, F.V., 1993, Isotopic evidence for preservation of Cordilleran lithospheric mantle during the Sevier-Laramide orogeny, western United States: Geology, v. 21, p. 719–722, https://doi.org/10.1130/0091-7613(1993)021<0719:IEFPOC>2.3.CO;2.

Luffi, P., Saleeby, J.B., Lee, C.-T.A., and Ducea, M.N., 2009, Lithospheric mantle duplex beneath the central Mojave Desert revealed by xenoliths from Dish Hill, California: Journal of Geophysical Research, v. 114, B03202, https://doi.org/10.1029/2008JB005906.

Miller, J.S., Glazner, A.F., Farmer, G.L., Suayah, I.B., and Keith, L.A., 2000, A Sr, Nd, and Pb isotopic study of mantle domains and crustal

structure from Miocene volcanic rocks in the Mojave Desert, California: Geological Society of America Bulletin, v. 112, p. 1264–1279, https://doi.org/10.1130/0016-7606(2000)112<1264:ASNAPI>2.0.CO;2.

Miller, N.C., and Behn, M.D., 2012, Timescales for the growth of sediment diapirs in subduction zones: Geophysical Journal International, v. 190, p. 1361–1377, https://doi.org/10.1111/j.1365-246X.2012.05565.x.

Porter, R., Zandt, G., and McQuarrie, N., 2011, Pervasive lower-crustal seismic anisotropy in Southern California: Evidence for underplated schists and active tectonics: Lithosphere, v. 3, p. 201–220, https://doi.org/10.1130/L126.1.

Spencer, J.E., Singleton, J.S., Strickland, E., Reynolds, S.J., Love, D., Foster, D.A., and Johnson, R., 2018, Geodynamics of Cenozoic extension along a transect across the Colorado River extensional corridor, southwestern USA: Lithosphere, v. 10, p. 743–759, https://doi.org/10.1130/L1002.1.

Strickland, E.D., Singleton, J.S., and Haxel, G.B., 2018, Orocopia Schist in the northern Plomosa Mountains, west-central Arizona: A Laramide subduction complex exhumed in a Miocene metamorphic core complex: Lithosphere, v. 10, p. 723–742, https://doi.org/10.1130/L742.1.

Torsvik, T.H., Müller, R.D., Van der Voo, R., Steinberger, B., and Gaina, C., 2008, Global plate motion frames: Toward a unified model: Reviews of Geophysics, v. 46, RG3004, https://doi.org/10.1029/2007RG000227.

Xia, H., and Platt, J.P., 2017, Structural and rheological evolution of the Laramide subduction channel in southern California: Solid Earth, v. 8, p. 379–403, https://doi.org/10.5194/se-8-379-2017.

Printed in USA